19th Brazilian Congress of Thermal Sciences and Engineering
November 6th–10th, 2022, Bento Gonçalves - RS - Brazil

ENC-2022-0503
EXPERIMENTAL STUDY OF FRACTURE-FILLING BY A NON-NEWTONIAN FLUID FLOW WITH PARTICULATE MATERIAL

Felipe B. Pereira
Cássio L. Schneider
Vinicius G. Poletto
Fernando C. De Lai
Research Center for Rheology and Non-Newtonian Fluid (CERNN), Federal University of Technology - Parana (UTFPR), Curitiba-PR, Brazil
felipepereira@utfpr.edu.br, cassioschneider@alunos.utfpr.edu.br, vinsptt19@gmail.com, fernandodelai@utfpr.edu.br

Alex T. A. Waldmann
André L. Martins
Leopoldo Américo Miguez de Mello Research and Development Center (Cenpes), Petrobras, Rio de Janeiro-RJ, Brazil
awaldmann@petrobras.com.br, aleibsohn@petrobras.com.br

Silvio L. M. Junqueira
Research Center for Rheology and Non-Newtonian Fluid (CERNN), Federal University of Technology - Parana (UTFPR), Curitiba-PR, Brazil
silvio@utfpr.edu.br

Abstract. *The presence of fractures, frequent in the reservoirs, together with the pressure gradients inside the wellbore, significantly accentuates fluid leakage into the rock formation. Adding LCM (lost circulation materials) to the drilling fluid is an alternative corrective method used to mitigate and control this issue. In the present work, we study the use of APU particles (abrasive plastic urea) acting as loss of circulation material combined with a non-Newtonian Herschel-Bulkley fluid to fill a fracture transversely located to a vertical channel. To characterize the lost flow rate, one built an experimental apparatus to monitor the pressure gradient caused by a valve opening at the end of the fracture. In general, using the APU solid particles combined with the non-Newtonian fluid is effective for treating the lost circulation problem. As the main finding, the addition of LCM particles with an average diameter of 0.363 mm to a Herschel-Bulkley fluid with an apparent viscosity of 10cP avoids the problem of loss of circulation by fully recovering the annular channel flow rate after suffering a fluid loss of 35%. Finally, results for the particulate beds formed during the fracture filling process and their respective geometries are also investigated.*

Keywords: *Fracture, Lost circulation materials, non-Newtonian fluid, Herschel-Bulkley.*

1. INTRODUCTION

The drilling process is characterized by the rotating movement of a drill that compresses and crushes the rock formation, generating a large number of fragments named cuttings. The hydrostatic pressure inside the wellbore is essentially associated with the drilling fluid. The drilling fluid is usually composed of a liquid phase with other materials that give the fluid non-Newtonian characteristics. One of the properties that significantly contribute to the increase of the wellbore hydrostatic pressure is the drilling fluid density, represented by an equivalent circulating density (ECD). The drilling process must occur under overbalanced conditions, where the ECD needs to be kept at a high enough value to maintain wellbore integrity, avoiding the fluid influx from the formation to the annular space, and lower enough to prevent a fracture induction (Caenn *et al.*, 2008). In high-depth reservoirs drilled under an overbalanced condition, the presence of fractures is very common. The fracture occurrences during the drilling process are usually an undesired phenomenon, as it promotes invasion of drilling fluid into the rock formation, characterizing the loss of circulation problem (Lavrov, 2016). The fluid loss is indicated by a decrease in the fluid flow rate that returns to the surface through the annular channel. The greater the fluid volume lost to the formation, the smaller the return of fluid to the surface through the annular region. The in-

tensifying fluid loss is extremely negative in many ocasions, since the process must be paralyzed to prevent the complete fluid loss (Howard and Scott, 1951). The time spent on maintenance increase the non-productive time (NPT) causing delays in production and monetary loss in the process. As a common situation in many wellbores being drilled nowadays, different techniques can be used to mitigate the fluid loss problem, the most common is obtained by adding particles of selected granulometry called LCM (lost circulation materials) to the drilling fluid. One of the purposes of LCM is to go through the preferential flow path created by the fracture and seal it preventing the fluid loss to the rock formation. A good non-Newtonian fluid and LCM mixture can result in large monetary savings in drilling processes. Recent studies based on field-collected data analysis reveal that the costs spent on treating loss of circulation reach approximately 12% of the total drilling costs (Feng and Gray, 2017). This value can represent the amount of 2-4 billion dollars annually. Therefore, the main objective of the present study is to evaluate the use of non-Newtonian fluids along with the LCM particulate materials to minimize the loss of circulation to fractures.

2. MATERIALS AND METHODS

The lost circulation phenomenon is characterized by a vertical channel, representing the annular space formed between the drill column and rock formation, with a rectangular cross-section that contains a transversal discontinuity to the flow region representing the fracture as can be seen in Figure 1. Figure 1(a) shows a schematic example of a drilling fluid invasion problem and Figure 1(b) shows a simplified geometry for the region of concern. The simplified region, it's important to notice, comprises only the representation of the annular region of the wellbore, that is, the region through which the drilling fluid returns to the surface. The drill's column internal region through which the drilling fluid is injected into the wellbore is not within the scope of this study. Furthermore, the fractured region is characterized by a discontinuity, and both the wellbore annular region and fracture's walls are considered impermeable. In this present work,

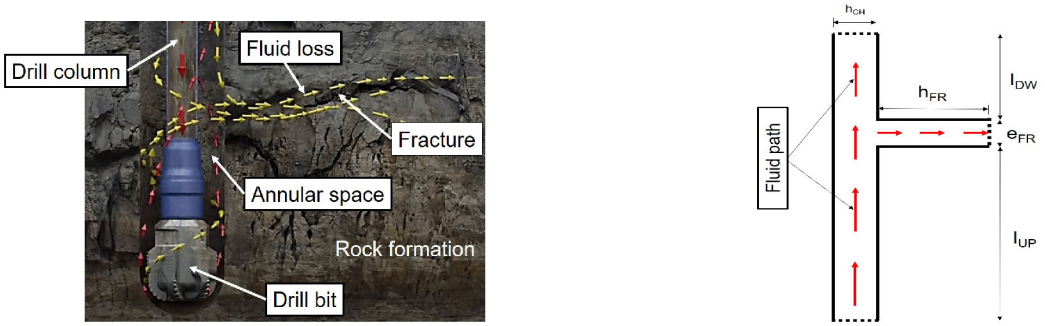

(a) (b)

Figure 1: Lost circulation phenomenon: (a) Schematic problem and (b) Simplified geometry.

the drilling fluid is represented by a mixture of a fluid phase (water) and an additive polymer that give it the behavior of a non-Newtonian fluid (Herschel-Bulkley fluid). A set of particles with selected granulometry characterizing the LCM is injected into the fluid to fill in the fracture and mitigate the fluid loss. As the LCM accumulates in the fracture region a porous bed is created and the fracture is obstructed decreasing the loss of fluid.

2.1 Experimental apparatus

The experimental apparatus comprises: a) a rectangular test section (E-3), b) an helical pump (E-2), c) a mixing tank (E-1), d) a mass flow rate meter (I-1), e) pressure transducers (I-3, I-4), d) an eletric control valve (V-2) and f) a temperature sensor (I-2). Figure 2 shows the experimental instruments disposition on a hydraulic system of apparatus.

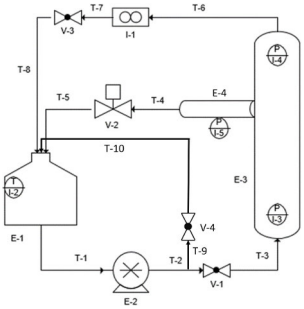

Figure 2: Apparatus hydraulic system disposition.

The rectangular test section (E-3), used in the experiments, is an adapted version of the project developed by Stahlke and Fritoli (2014) and modifications of Schneider (2016). This test section is made of acrylic, a translucent material that allows the fluid-particles interaction visualization. The test section has two meters long and it's composed of an internal channel with a rectangular cross-section with a 16mm width (h_{CH}) and depth of 45mm as can be seen in Figure 3. The h_{CH} dimension represents the wellbore annular region size in a certain stage of the drilling process with an internal diameter of 5 inches and an external diameter of 8.5 inches (Calcada *et al.*, 2015). The discontinuity at E-3 is highlighted green in Figure 3 and characterizes the discrete fracture (E-4) located at a distance of 1.27m from the vertical channel inlet.

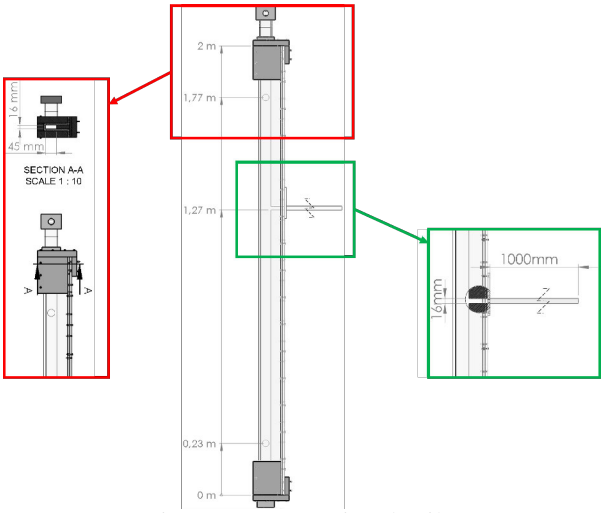

Figure 3: Test section details.

The data acquisition system from the pressure, the flow rate meter, and the temperature transducers are made via 485 communication to LabVIEW software and are stored and exported to Microsoft Excel spreadsheets. The acquisition is done through a National Instruments board. The apparatus comprises a chassis and three modules where two it is for the input and one is for the output which is responsible for sending and receiving data from the equipment. The chassis model is the cDAQ-9174 with a capacity of four modules. Figure 4 represents the experimental apparatus disposition in the laboratory premises.

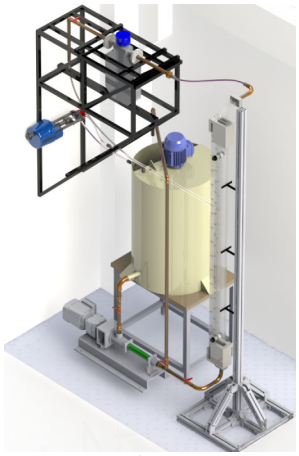

Figure 4: Experimental apparatus.

2.2 Lost ciculation materials - LCM

The LCM used in the present work has a function to interact with the non-Newtonian fluid so the flow rate loss, Q_V, through the fracture E-4 becomes effectively minimized without significant pressure changes in the wellbore region. For this purpose, the granulometry and particle mass concentration were evaluated. The LCM was selected based on experimental work carried out by Fritoli (2018), Pereira (2019), and Schneider (2019). Among the types of particulate materials that could be used, three different granulometry of urea plastic abrasive (APU) were chosen. These abrasives are commonly used in blasting applications to remove old paint, hard cleaning, and remove coatings and paint from aircraft. The APU has a Barcol hardness range that can vary from 54 to 62, and was acquired from the Zirtec company, has an

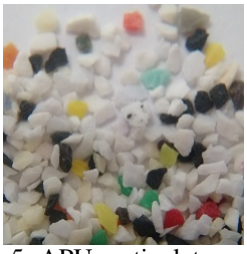

Figure 5: APU particulate material.

Table 1: Particulate material characteristics.

Characteristics	Values
Specific mass	1,6 g/cm^3
Urea 40-60	0,25 <dp$_1$< 0,42 mm
Urea 16-20	0,08 <dp$_2$< 1,2 mm
Urea 12-16	1,19 <dp$_3$< 1,68 mm
Color	Merged white
Barcol hardness	54-62

opaque and irregular appearance with a mixed coloration as shown in Figure 5. The granulometry ranges used can be seen in Table 1, where "dp" refers to the particle diameter of LCM.

2.3 Fluids formulation

To evaluate the viscosity influence in the experiments were used two formulations with different concentrations of carbopol (CBP) in water provided apparent viscosities values of approximately 10cP, and 20cP for the shear rate of $1000s^{-1}$. The results are compared concerning the standard fluid apparent viscosity which in this case was the CBP formulation with a viscosity of 10cP for the shear rate value equal to $1000s^{-1}$.

To obtain the fluids flow curves, the FANN® model 35A (FANN, 2016) rotational viscometer was used, which can be seen in Figure 6. The viscometer is a piece of equipment more robust than conventional rheometers but way more imprecise. However, for this study, it would not be necessary to have equipment with precision as refined as like a rheometer and it was decided to use viscometer equipment that is easy to handle and has better portability. Furthermore, this equipment can be used in the field applications of the drilling process and allows the operator to make a quick decision regarding the type of additive to be added into the drilling fluid to obtain the desired apparent viscosity.

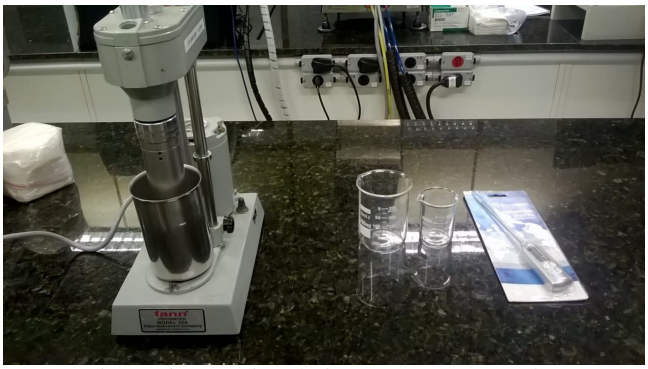

Figure 6: Rotacional viscometer FANN 35A.

In this viscometer, the fluid is contained in the annular space formed between an outer cylinder where the fluid sample is placed and the inner cylinder (plumb). Viscosity measurements are made when the outer cylinder rotates with a defined velocity, causing a viscous drag exerted by the fluid. This drag creates a torque on the inner cylinder which is transmitted to a precision spring where its deflection is measured (FANN, 2016). This viscometer model has six different operating speeds, which range from 3rpm to 600rpm and each rotation speed provides a certain value for the deflection angle which is used to obtain the shear stress and strain values, that can be easily obtained by equations (1) and (2) respectively.

$$\tau = \frac{K_1 K_2 \Theta}{10} \tag{1}$$

$$\cdot\gamma = K_3 N \tag{2}$$

where K_1 is the torsional constant, K_2 is the shear stress for the effective surface of the inner cylinder, K_3 is the strain constant, θ is the deflection angle, and N is the number of revolutions of the outer cylinder. The values of the equipment's constants are displayed in the Table 2. Table 3 presents the list of fluids that are used in the experimental tests of this study. The apparent viscosity value (η) refers to the measured viscosity at a shear rate equal to $1000s^{-1}$.

Table 2: Viscometer constant values.

Constant	Value	Unit of measurement
K_1	300	$dina.cm/^\circ$
K_2	0,01323	$1/cm^3$
K_3	1,7023	$1/s.rpm$

Table 3: Formulated fluids.

Fluid	Formulation	η	Polymer [%]
CBP10	water + gel	10	15%
CBP20	water + gel	20	20%

3. RESULTS

Table 4 summarizes the experimental parameters and their respective variation values. The standard values used for the comparison with the variations are highlighted in Table 4.

Table 4: Parameters variation values.

Parameter	Symbol	Value	Unit of measurement
Flow rate loss	Q_V	5, 10, 20, **35**, 50	[%]
Reynolds number	Re	100, **200**, 300	[-]
LCM mass percentage	%LCM	1, 2, **3**	[%]
Granulometry	dp	0,363; **1,09**; 1,4	$[mm]$
Apparent viscosity	η_{1000}	**10**, 20	$[cP]$

3.1 Fracture filling standard experimental procedure

After the fluid has been properly formulated the LCM with an intermediate dp_2 granulometry is added to it at a standard value of 3% which represents a mass of 1,021kg. After the LCM addition to the mixing tank, the flow rate is adjusted so that the Reynolds number through the vertical channel (that represents the wellbore annular space) can be reached. This flow adjustment is carried out through the LabVIEW software. Once the non-Newtonian fluid is formulated and the flow curve is found, the rheological parameters obtained are placed into the Reynolds number equation in the LabVIEW and the system is remotely activated starting the flow. The flow rate through the vertical channel is modified until the correct Reynolds number is obtained. Once the Reynolds number is reached the test begins. The test starts with the fracture completely closed. At the time of 100s, the control valve is activated and the fracture is opened to obtain a defined flow rate loss of Qv = 35%. In the moments following the fracture opening the flow rate that returns, through the vertical channel to the mixing tank, decreases abruptly to the point of a minimum flow rate measured which characterizes the overshoot that corresponds to the highest fluid flow rate loss (fluid flow rate loss of reference) obtained. Figure 7 shows the results for the fluid flow rate loss over time obtained in the tests, in which Figure 7(a) shows the flow rate loss behavior, and Figure 7(b) shows the results for differential pressure in the fracture over time. Shortly after the fracture opening, the fluid flow rate loss increases from zero to the maximum flow rate loss value (35%). After that, the solid particles begin to deposit sealing it and decreasing the flow rate loss to the fracture.

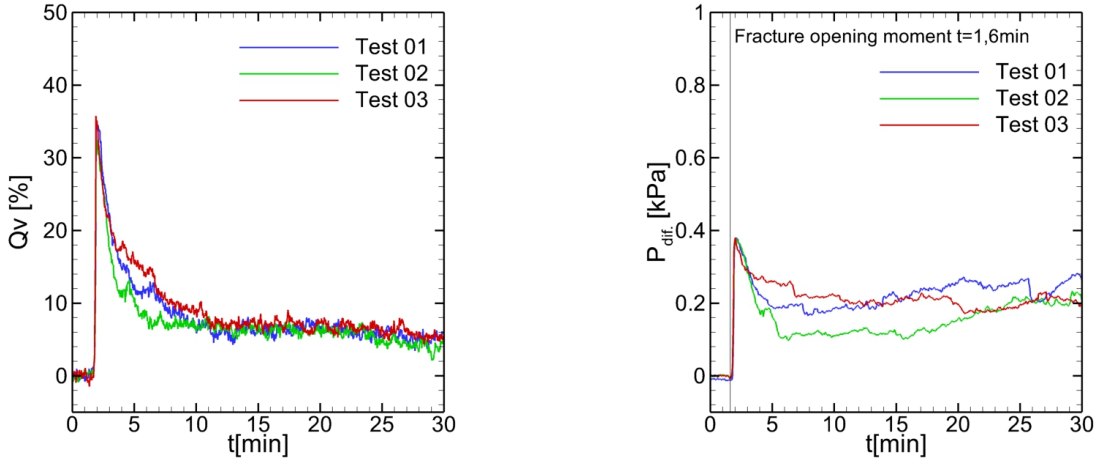

(a) (b)

Figure 7: Results for (a)flow rate loss and (b)fracture diferenttial pressure through time.

Figure 8 shows the particulate bed formation evolution over time in the fractured region. The images of the beds in Figure 8 comprehend the free rectangular channel region on the picture's right side and the fracture entry region (approximately 300mm in length). The instant of 0s corresponds to the instant that precedes the fracture opening and there is no flow through the fracture yet. Before the opening, some particles close to the fracture inlet next to the vertical channel wall, where the flow speed is close to zero m/s, accumulate on top of each other creating a barrier at the entrance to the fractured region as can be seen in Figure 8 at t=0s. After the opening, the particles begin to be carried by the fluid into the fracture where it starts to create a particulate bed.

Figure 9 shows the results for the final LCM beds formed across the triplicate tests of the fracture fill with default settings. As we can notice, the particles bed layer formed had the same length for the three tests since the experimental

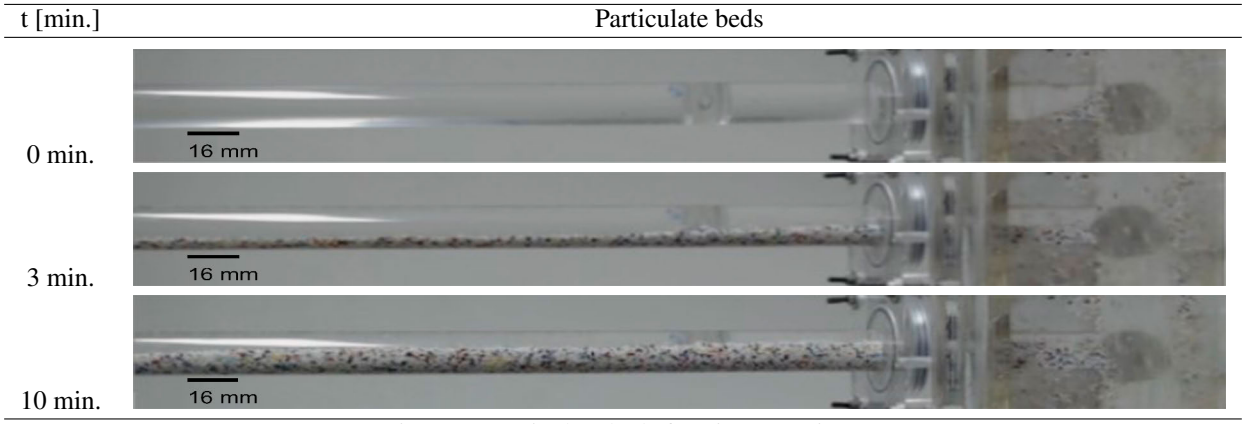

Figure 8: Particulate beds forming over time.

parameters were the same in all cases.

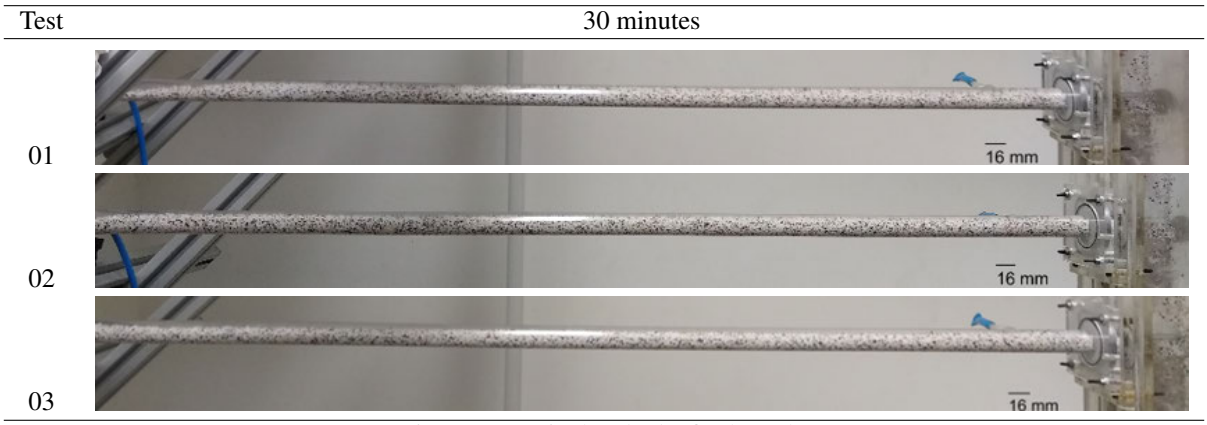

Figure 9: Particulate bed's final result.

3.2 Flow rate loss through fracture variation influence - Q_V

The flow rate through the fracture (Q_V) was varied in five different values keeping the other parameters fixed. Figure 9 shows the results for Figure 9(a) flow rate loss Q_V and Figure 9(b) fracture differential pressure through the time. Before the fracture opening, the flow rate loss is equal to zero and once the fracture is open the fluid immediately invades the fracture and the fluid loss reaches its maximum value. As the solid particles start to deposit into the fracture, the fluid loss rate decreases. Figure 9(b) shows that the greater the flow rate loss, the bigger the pressure in that instant. For the lowers values of Q_V the pressure is lower as well, and besides that don't have a large behavior variation as for the other cases. In fact, for the lower Q_V the particulate beds formed are created much more slowly that's why the fracture differential pressure in that cases has a slight variation. For the higher Q_V value the particles invade the fracture faster and quickly arrive at the fracture outlet where there is a mechanical obstruction (a control valve) that holds the LCM particles. So, the flow rate through the fracture is decreased quickly and the particle bed is created slowly. That's why the pressure variation, in that case, was smaller than the other with Q_V equals 35%.

The particle beds formed in the experimental tests for each flow rate loss variation can be seen in Figure 10. We can notice that the volume of solids inside the fracture has a determinant influence on the differential pressure values. For the 05% and 10% flow rate loss through the fracture, we can see a small numuber of particles on the fracture inlet and then a small layer of particles until the outlet. The same situation occurs for the higher flow rate loss (50%) except for the large volume of LCM on the fracture entrance region. But, in these cases, the pressure has practically the same behavior (nearly constant variation) over the entire experiment. For the intermediary flow rate values (20% and 35%), the volume of LCM inside the fracture is very high, creating a porous layer (or bed) from the inlet to the fracture outlet. That provides a slow growth for the LCM layer and a larger differential pressure variation over time.

The results of the fractures filling on the fluid flow rate loss variation can be seen in Table 5 which shows the initial flow rate in the annular ($\overline{Q}_i$), the minimum flow rate (Q_{min}), the flow rate loss (Q_V), the final flow rate in annular ($\overline{Q}_f$) the reestablished flow rate percentage ($\overline{Q}_f/\overline{Q}_i$).

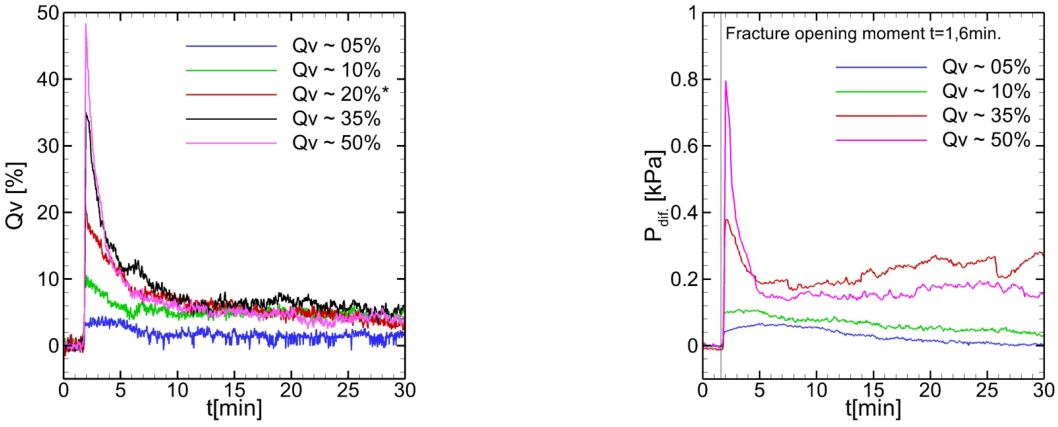

(a) (b)

Figure 10: Results for (a)flow rate loss and (b)fracture diferenttial pressure through time.

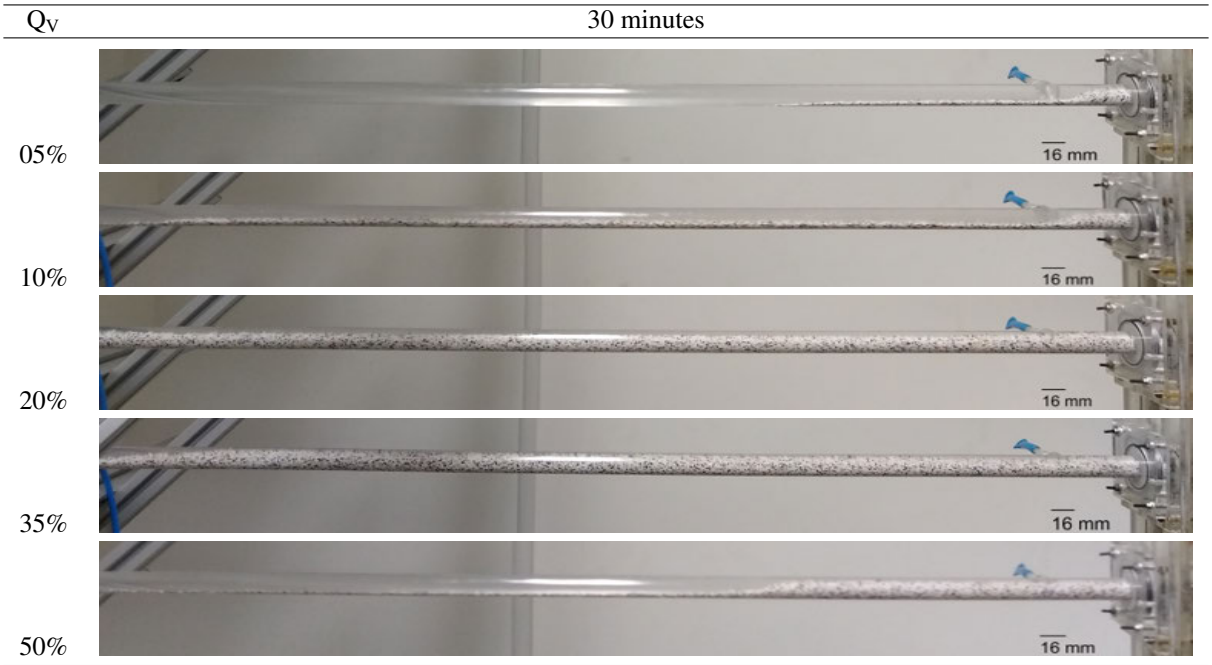

Figure 11: Particulate bed's final formation results.

Table 5: Flow rate values from the experimental tests.

Q_V [%]	$\overline{Q}_i$ $[m^3/h]$	σ_{Q_i}	Q_{min} $[m^3/h]$	$\overline{Q}_f$ $[m^3/h]$	σ_{Q_f}	$\overline{Q}_f/\overline{Q}_i$ [%]
05	0,440	0,001	0,421	0,435	0,004	98,69
10	0,441	0,002	0,394	0,420	0,002	95,26
20	0,438	0,003	0,344	0,419	0,004	95,81
35	0,431	0,002	0,280	0,407	0,003	94,25
50	0,444	0,002	0,229	0,427	0,003	95,94

3.3 LCM granulometry variation influence

The LCM granulometry was changed to show the particle size influence on the fluid loss mitigation. Keeping the stardard parameters fixed, was used three different particles granulometry ranges as can be seen on Table 6.

Changing the particle's granulometry implies a change in the volume of solids on the flow to guarantee the same mass concentration for the three cases. So, for the dp_1 urea particles granulometry the flow has a higher volume of individual particles interacting with each other. Figure 12 shows the plot results for Figure 12(a) fluid flow rate loss through the fracture and Figure 12(b) fracture differential pressure over time. For all the cases the maximum Q_V is equal to 35% of loss as this is a fixed parameter. Figure 12(a) shows the great influence that the smaller particle size has on the flow. Almost immediately after the fracture opening the LCM particles seal it very fast not letting the fluid loss evolve. While

Table 6: Particles granulometric parameters values.

LCM	Granulometric ranges informed $[mm]$	Average measured values $[mm]$
Urea 40-60	0,25 < dp_1 < 0,42	dp_1 = 0,363
Urea 16-20	0,8 < dp_2 < 1,2	dp_2 = 1,09
Urea 12-16	1,19 < dp_3 < 1,68	dp_3 = 1,4

for the other cases the fluid loss decreases more slowly and even then it does not completely seal the fracture. From Figure 12(b) can be expected a small volume of solids inside the fracture since the differential pressure for this case there wasn't a high variation in behavior.

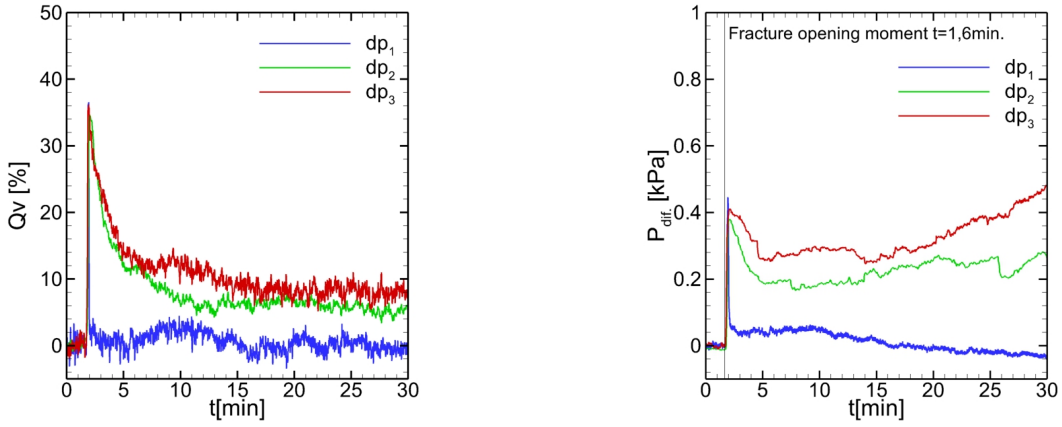

(a) (b)

Figure 12: Results for (a)flow rate loss and (b)fracture diferenttial pressure through time.

Table 7 shows the fluid flow rate final values for the granulometry variations. As expected, the particles bed formed from dp_1 granulometry has less volume of solid than the others as can be seen in Figure 13.

Table 7: Flow rate values from the experimental tests.

LCM	$\overline{Q}_i$ $[m^3/h]$	σ_{Q_i}	Q_{min} $[m^3/h]$	Q_V $[\%]$	$\overline{Q}_f$ $[m^3/h]$	σ_{Q_f}	$\overline{Q}_f/\overline{Q}_i$ $[\%]$
dp_1	0,431	0,005	0,273	36,54	0,431	0,004	100
dp_2	0,431	0,002	0,280	35,10	0,407	0,003	94,25
dp_3	0,429	0,004	0,274	36,18	0,394	0,004	91,91

For the LCM with dp_2 and dp_3, the particles have double and triple the size of dp_1 respectively, so the beds formed by those solid particles have a higher porosity that helps the flow keep going through the fracture but non-stopping the fluid loss. So, as shown in Table 7 the LCM with dp_1 is more efficient in mitigating the loss of fluid.

3.4 Apparent viscosity influence

The last parameter to be varied was the fluid's apparent viscosity. For this purpose except for CBP, which was modified in concentration, the other parameters were kept fixed. Two different CBP concentrations were used to modify the fluid's apparent viscosity, resulting in a fluid with 10cP and another with 20cP, as shown in the plots of Figure 14, where Figure 14(a) is the flow curve and Figure 14(b) the apparent viscosity curve.

The fluid's parameters were obtained from the Herschel-Bulkley model Eq. (3) and can be seen in Table 8:

$$\begin{aligned} \tau_{yx} &= \tau_{0_{HB}} + m\dot{\gamma_{yx}}^{n} \quad for \quad |\tau_{yx}| > |\tau_{0_{HB}}| \\ \dot{\gamma_{yx}} &= 0 \qquad\qquad\quad for \quad |\tau_{yx}| < |\tau_{0_{HB}}| \end{aligned} \tag{3}$$

where $\tau_{0_{HB}}$ is the Herschel-Bulkley yield stress [Pa], n is the power law index and m is the consistency index. After the appropriate fluid formulation been set, the experimental tests starts.

Figure 15 shows the results for flow rate loss, Figure 15(a), and fracture differential pressure, Figure 15(b), through time. After opening the fracture and the flow loss reaching the maximum value, the flow with CBP20 reduces the fluid loss faster than CBP10 fluid. That happens because a huge quantity of particles is taken through the fracture very fast obstructing the fracture outlet. For CBP10 this does not happen faster enough because the fluid has a lower viscosity and the particles take more time to deposit in the fracture. The pressure in the fracture for the CBP20 is greater than the

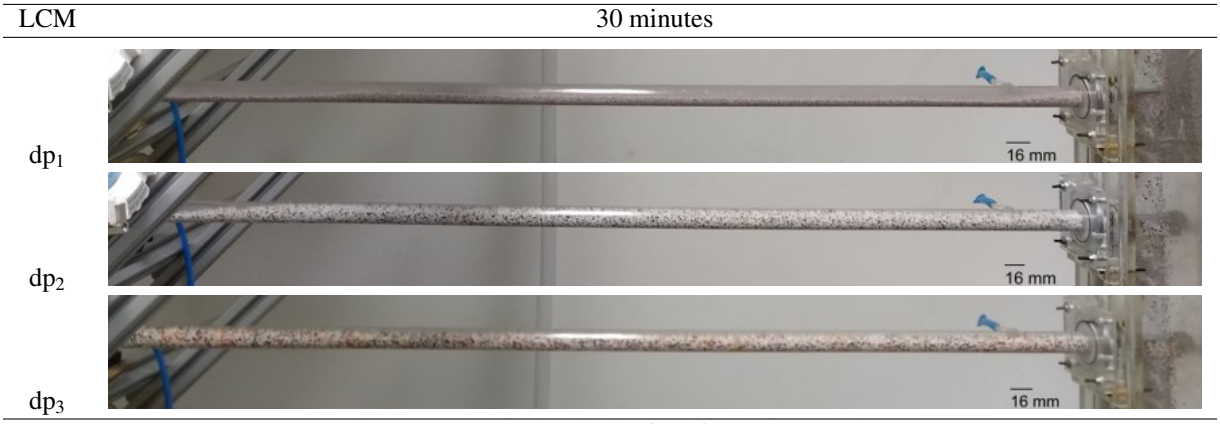

Figure 13: Particulate bed's final formation results

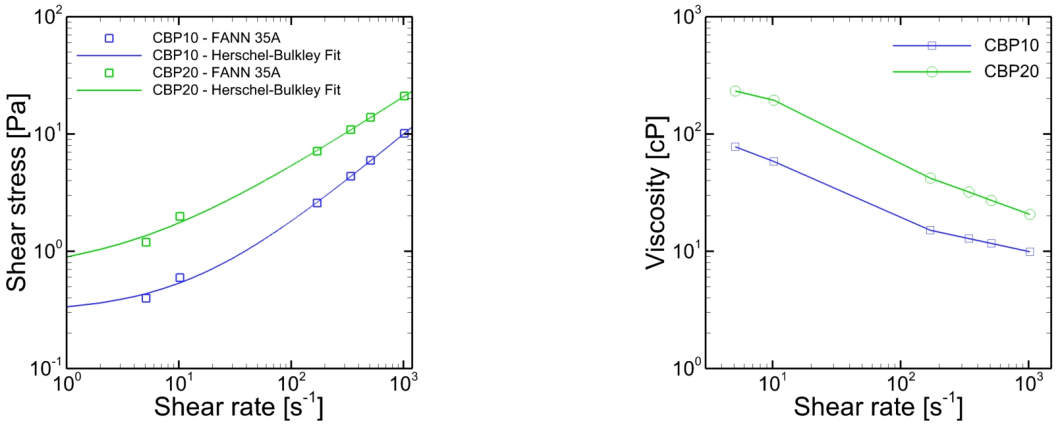

(a) (b)

Figure 14: Rheology curves: (a)Flow curves and (b)Viscosity curves.

Table 8: Fluids rheological values.

Fluid	$\tau_0[Pa]$	$k[Pa.s^n]$	$n[-]$	$\eta_{1000}[cP]$
CBP10	0,2981	0,03716	0,805	9,90
CBP20	0,6326	0,26280	0,620	20,50

CBP10 at the moment the fracture opens because the fluid is heavier. But from the moment the LCM starts to fill the fracture the pressure stabilizes and has a small variation in behavior. Following the pressure plot, we can expect that the flow with CBP20 has a smaller volume of solids in the fracture than the CBP10. We can see this in Figure 16, which shows the final results for the particles bed created.

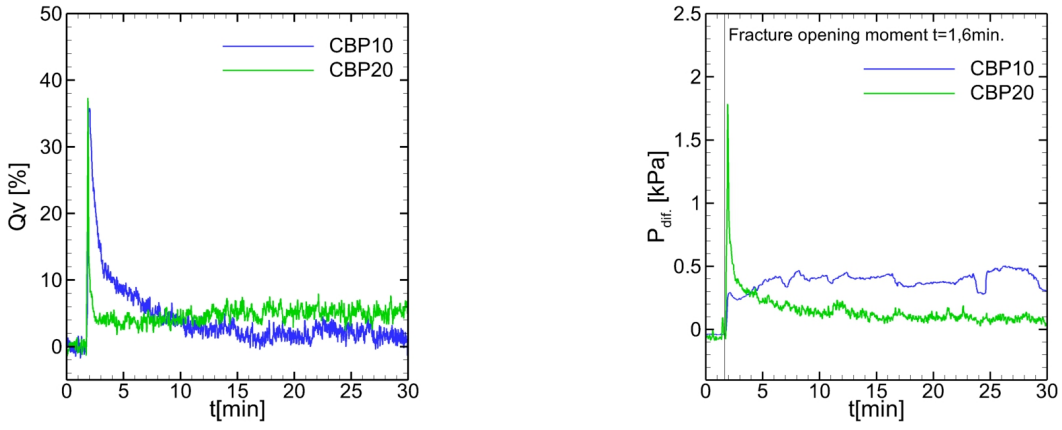

(a) (b)

Figure 15: Results for (a)flow rate loss and (b)fracture diferenttial pressure through time.

Fluid	30 minutes
CBP10	
CBP20	

Figure 16: Particulate bed's final formation results.

4. CONCLUSIONS

In the present work, the combination of particulate material with non-Newtonian Herschel-Bulkley fluid flow to fill fractures has been experimentally studied. The experiments aimed to investigate the possibility of mitigating fluid loss through a transverse fracture of a vertical channel subject to loss of circulation. The analysis considered combinations of Herschel-Bulkley fluid with solid particles of varying granulometry. The main findings of the present work can be summarized as:

- Variations in the flow rate lost through the fracture indicate the flow velocity and the volume of solids within the fracture highly affect the differential pressure.
- Smaller particles ranging from 0,25 to 0,42mm can entirely seal the fracture.
- Higher viscosities do not mean efficient fracture sealing, as observed from the results where the CBP20 fluid had a more significant loss across the fracture.

5. REFERENCES

Caenn, R., Darley, H. and Gray, G.R., 2008. "Drilling problems related to drilling fluids". In *Composition and Properties of Drilling and Completion Fluids*, Gulf Professional Publishing, pp. 367–460.

Calcada, L.A., Duque Neto, O.A., Magalhaes, S.C., Scheid, C.M., Borges Filho, M.N. and Waldmann, A.T.A., 2015. "Evaluations of suspensions flow and particlulate materials for control of fluid losses in drilling operations". *Journal of Petroleum Science and Engineering*, Vol. 131.

Feng, Y. and Gray, k., 2017. "Review of fundamental studies on lost circulation and wellbore strengthening". *Journal of Petroleum Science and Engineering*, p. 12.

Fritoli, G., 2018. *Avaliação experimental do processo estático de formação de reboco particulado em filtro prensa API.* Master's thesis, Universidade Tecnológica Federal do Paraná, Curitiba.

Howard, G. and Scott, P., 1951. "An analysis and the control of lost circulation". *Journal of Petroleum Technology*, Vol. 3, No. 1, pp. 171–182.

Lavrov, A., 2016. *Lost Circulation*. Gulf Professional Publishing, Massachusetts, USA.

Pereira, F.B., 2019. "Análise do escoamento particulado com fluido não newtoniano em canal vertical".

Schneider, C.L., 2016. *Estudo Experimental do Preenchimento de Fraturas com Escoamento Particulado em Canal Fraturado*. Master's thesis, Universidade Tecnológica Federal do Paraná, Curitiba.

Schneider, C.L., 2019. *Estudo Experimental da perda de circulação de fluidos não newtonianos em meios porosos fraturados*. Master's thesis, Universidade Tecnológica Federal do Paraná, Curitiba.

Stahlke, B.R. and Fritoli, G.S., 2014. "Projeto e construção de bancada experimental para o estudo de escoamento particulado em canal fraturado".

6. RESPONSIBILITY NOTICE

The authors are solely responsible for the printed material included in this paper.